Chapter 20
Interaction Effects between Strip and Work Roll during Flat Rolling Process

S. Puchhala, M. Franzke, and G. Hirt

Abstract. During the flat rolling process (cold or hot), the strip flatness and thickness profile are highly influenced by the interaction effects between strip and work rolls. To understand and analyze these effects a new modeling concept was developed. Within this concept, the tool simulations are separated from the process simulation. With the help of an automatic coupling module, the influences of the tool effects are realized within the process simulation. With this modeling concept, three types of interaction phenomena are studied and validated using experiments: elastic roll effects during the cold rolling process, work roll thermal effects during the hot rolling process and tribological effects (abrasive wear) on the process simulation. It was also shown that, compared to the single FE model, this modeling concept is relatively faster and suitable for large 3D models without losing the quality of the predicted results.

20.1 Introduction

During the flat rolling process, the dimensional tolerances and the mechanical-metallurgical properties of the rolled products become more stringent. Therefore, computational models are being used to investigate the physical aspects, such as thermo-mechanical events of the strip, mechanical deformation and thermal evolution of the work rolls, and tribological effects, such as wear. Conventional numerical modeling of such processes assuming plane strain conditions (2D) may not be sufficient since the contact pressure distribution along the strip width may have a non-uniform profile due to the elastic deformation of the work rolls. Depending on the roll elastic deformation, strip flatness profile changes, i. e. crowns, will originate (see Fig. 20.1). The modeling of such processes using a conventional single FE model and considering all the above-mentioned effects, will not only complicate the computation (deformable – deformable contact situation has to be handled) but also affect the computation time. This situation is even more complicated when contact between elastic tools (in the case of backup rolls) has to be considered.

Significant effort was devoted to the study of mechanical and thermo-mechanical effects in the strip and work rolls using the numerical methods. Particularly, A. Kainz [1] simulated a skin pass cold rolling process (in 2D) considering elastic effects of the work rolls using the commercial FE program

B. Denkena and F. Hollmann (Eds.): Process Machine Interactions, LNPE, pp. 439–458.
springerlink.com

ABAQUS/EXPLICIT. He stated that, for the computation of 22 ms (150 mm strip length) of real process time, simulation required several days. On the other hand, T.H.Kim, S.M.LEE [2] presented an integrated FE process model, where the strip profile was analyzed using 3D implicit simulations. However, the mechanical contact computations (at strip-work roll and work roll-backup roll interface) are handled using analytical models and coupled with individual FE simulation models. Several other researchers [3, 4, and 5] have presented the modeling of cold rolling processes considering elastic work rolls using single FE models in 2D configurations. A fully-coupled 3D FE simulation of the cold rolling process (considering the roll flattening and bending effects) is yet to be realized.

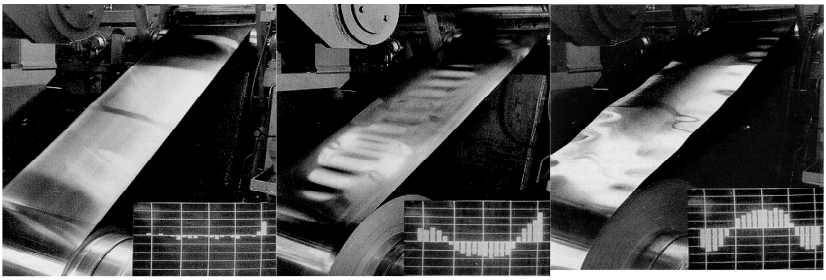

Fig. 20. 1 Strip profile quality problems during cold rolling process

For the modeling of a hot rolling process, Tseng [6] simulated steady state heat transfer in the work roll using a two-dimensional Finite Difference Method. Using an empirical approach, he included the heat generation term due to plastic deformation and friction between roll and strip. On the other hand, Hsu and Evans [7] conducted a two-dimensional FE analysis of the rolling process considering a steady state heat transfer condition. C.G.SUN and S.M.HWANG [8,9] presented integrated models considering the thermo-mechanical effects both in roll and strip for 2D and 3D. They presented a coupled model for the hot rolling simulation, where they considered the steady state heat transfer using 2D models for the rolls. They also considered the elastic deformation of the work rolls. LEE and Hwang [10] presented a similar model for the computation of the thermal effects for the work rolls. These models have been validated with the experimental results and are good for the estimation of the thermal behavior of the rolls during a hot rolling process. The only untouched area in those models is the analysis of bi-directional interaction effects between strip and rolls.

At the same time, during cold and hot rolling processes, the tribological events, particularly abrasive wear of the work rolls, directly affect the rolled strip surface quality and may hinder the flatness profile [11, 12]. Many investigations have been carried out to understand the wear mechanism of the rolls during rolling processes [13,14,15,16]. All of these studies are related to the modeling of wear using analytical methods or empirical models. As far as we know, offline calculations of precise local work roll wear during hot or cold rolling have not yet been noticed.

The objective of this work is to develop a validated simulation tool for the analysis of the interaction effects between the work rolls and the strip during a flat rolling process. For that, a novel FE modeling concept was developed considering three different aspects, which influence the strip quality, i. e. elastic effects of the work rolls during a cold rolling process, thermo-mechanical effects of the work rolls during a hot rolling process and work roll tribological effects (mainly abrasive wear) during cold and hot rolling processes. In the following sections, each of these aspects is discussed in detail. In the next section, a detailed description of the de-coupled modeling concept (applicable for the modeling of all three aspects mentioned above) is explained. The details of abrasive wear models and their implementation are also discussed within the next section. In the section "modeling and analysis of a cold rolling process with elastic rolls", the cold rolling experimental setup and the optical deformation measuring method is explained. Later, the FE modeling of the cold rolling process using the new modeling concept is described; and the simulation and experimental results are given in a sub-section. In the section "modeling and analysis of hot rolling process", an identical structure as mentioned above is maintained. In the following section, the modeling of work roll wear is described. At the end, a detailed discussion on the overall work (modeling concept and the results) is given.

20.2 Concept and Implementation

A numerical simulation strategy was developed using FEM to analyze the interaction effects during rolling processes. Within this concept, the computation of the flat rolling process simulation is separated into two simulation models. In this context, the process simulation model consists of the workpiece (modeled using elastic-plastic material description for cold rolling and thermo-mechanical description for hot rolling) and the work rolls were modeled as rigid bodies (see Fig. 20.2). On the other hand, a different simulation model is considered for the tools (pure elastic model in case of cold rolling and thermo-mechanical model in case of hot rolling). These two separate models are coupled using an automatic-update module. This module uses a mapping table (where the FE surface mesh information of both rigid and elastic tools is saved) to update the geometrical information in both simulation models. For the communication and compatibility between two simulation models, an identical surface mesh is to be used in both models. Further details of the concept, such as data transfer, tool activation and mesh compatibility (Do Elastic Tool Simulation DOELTOSIM module), are described in the [19].

Based on this modeling concept, two other technical aspects were implemented: thermo-mechanical tool effects and wear prediction. For the modeling of a hot rolling process, consideration of the tool thermo-mechanical effects are very important since a large amount of the energy is conducted into the work rolls, when they come in contact with the hot strip. Here, the computation of roll thermo-mechanical effects is separated from the process simulation model. At each pre-defined time step, the computation of tool effects is activated. In case of 10 Sec total simulation time, if the pre-defined time step size is 2 Sec, the tool simulation is activated 5 times. As the thermal effects are transient, unlike the elastic

simulation model, the thermo-mechanical tool computation is carried out simultaneously until the next activation takes place. As the process and tool simulation models run concurrently, the tool simulation results should be readily available once the process simulation reaches the activation time-step. For that, a novel concept of rotating boundary conditions was developed to avoid the accumulation of large rotations of the Lagrange mesh of the work roll.

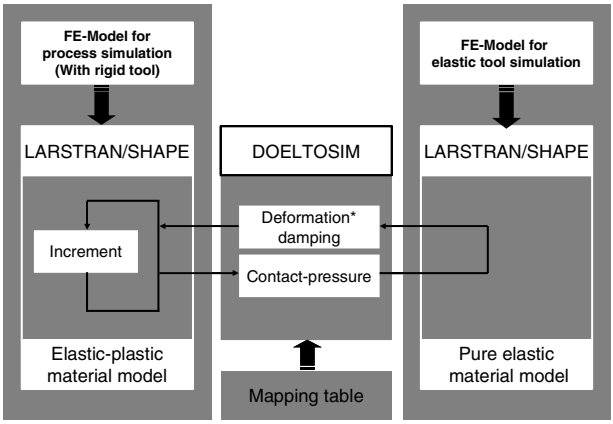

Fig. 20. 2 FEM-FEM coupling concept

Within this concept, the work roll is fixed in all DOF (Degrees Of Freedom) and the boundary conditions, such as heat flux at roll-strip contact, cooling zones are defined as rotating (with the rolling velocity) boundary conditions (see Fig. 20.3).

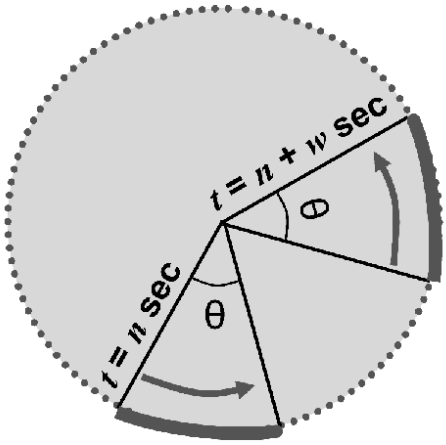

Fig. 20.3 Concept of rotating boundary condition

The conductive heat flux (at roll - strip contact zone) is calculated using the state variables (contact pressure and strip temperature) provided by process simulation (Eq. 20.1).

$$q = h_{gap}(T_{strip} - T_{roll}) \tag{20.1}$$

The gap conductance h_{gap} is defined as a function of contact pressure, roll roughness and roll hardness. Detailed explanation of this model is given in the section "modeling and analysis of hot rolling". In the same way, the convective heat fluxes (due to water cooling and air cooling) are calculated using Equations 20.2 and 20.3.

$$q = h_{water}(T_{roll} - T_{water}) \tag{20.2}$$

$$q = h_{air}(T_{roll} - T_{air}) \tag{20.3}$$

For the application of conductive heat flux, the contact angle θ is necessary and approximated using the contact length (l'_d) and deformed roll radius (r') as shown in Equation 4.

$$\tan\theta = \frac{l'_d}{r'} \text{ with}$$
$$r' = r(1 + C_H \frac{F}{b\Delta h} \text{ and } l_d = \sqrt{r'\Delta h} \tag{20.4}$$

The last aspect considered to analyze the interaction effects is work roll wear. It is known that the rolled strip profile will have the roll gap contour, i. e. if the work rolls are worn, the roll gap contour will no longer be uniform. Hence, it is important to analyze the wear progress of the work rolls during the rolling process. To analyze the local abrasive wear of the work rolls, three different wear models were selected and are coupled to the FE process simulation similar to the concept shown in Figure 20.2. The first model is the basic Archard model [15], where the wear depth is a function of normal forces F_N, hardness of the softer surface H , the sliding distance s and wear coefficient k (Eq. 20.5). The basic assumption of this model is that the wear rate is independent of the apparent contact area; and it also makes no considerations of variations with time. Moreover, this model is widely used since it provides a good estimation for the order of magnitude with less effort.

$$\frac{V}{s} = k\frac{F_N}{H} \tag{20.5}$$

The second model is an empirical model, which is a modified version of Oike's equation [18], which is tailored for the hot rolling process (Eq. 20.6). This model was developed and is being used for the on-line observation of wear for the finishing stands of a hot strip mill at TATA steel, India. Within the equation, the most important process parameter is the contact pressure P and other parameters, e. g. w_{strip} is strip width, l_d is contact length, Δh is the thickness reduction, L_{strip} is the length of the rolled strip and R is the radius of the work roll. The empirical constants α, β and γ were determined using a stochastic optimization technique,

i. e. the summation of wear error (difference between maximum measured wear and predicted wear) should be minimum. For the rolling of high carbon steels with 30 % thickness reduction, the wear coefficients were predicted as 1.0E-10, 0.188 and 0.11 respectively.

$$W(x) = \alpha \frac{L_{strip}}{2\pi R} \left(\frac{P}{w_{strip} l_d} \right)^{\beta} (l_d \Delta h)^{\gamma} \tag{20.6}$$

Within the last wear model, energy dissipation is introduced into the Archard's wear model (K.E. Nürnberg [14]) leading to reasonable qualitative wear prediction. By applying the Coulomb law to the Archard equation (Eq. 20.7) the dissipation rate is defined as the product of shear stress τ (MPa) to the sliding velocity v (mm/s). From Equation 20.8, the rate of wear and wear work Z can be directly related to the frictional dissipation rate. At the same time, the accumulated wear work is directly proportional to the dissipated energy. Finally, the wear model at element level can be written as a function of the accumulated wear work Z_{acc} and the contact pressure (as shown in Eq. 20.9).

$$w = \frac{k}{H} \int p v_t dt = \frac{k}{H} \int \mu \tau_t v_t dt \tag{20.7}$$

$$\dot{D} = \tau_t v_t \quad \Rightarrow \quad Z = \mu \int \dot{D} \tag{20.8}$$

$$w_e(r) = \frac{k(Z_{acc,e})}{H} \int p_e(r,t) v_{slid}(r,t) dt \quad where \; Z_{acc} = \sum_{r=1}^{n} Z_e \tag{20.9}$$

20.3 Modeling and Analysis of Cold Rolling Process

In general, the cold rolling process is carried out at the final stages of the rolling process, i. e. no other forming process step is conducted, which has an impact on the thickness profile in a corrective manner. On the other hand, the thickness profile has a substantial influence on the following forming processes, i. e. deep drawing process. The thickness profile directly depends on the contact pressure distribution along the roll gap. Due to elastic deformation of the work rolls an inhomogeneous contact pressure distribution may develop.

Table 20.1 Process and geometric parameters for the cold rolling process

Parameter	**Value**
Initial strip thickness	1.67 mm
Exit strip thickness	1.65, 1.48, 1.22, 1.20 mm
Work roll radius	300 mm
Work roll velocity	200 mm/sec
Friction coefficient	0.3
Strip tension (front and back)	30 kN

To obtain a deep understanding of the plastic flow of the strip and elastic deformation of the work rolls, implicit FE simulations were performed utilizing the newly-developed concept. As described in the implementation section, the process simulation model consists of a strip with elastic-plastic material description; and the rolls are considered as rigid bodies. Four different thickness reduction cases were simulated. Since the contact length for each case is not higher than 10 mm, at least 20 elements (with 0.5 mm length for both strip and roll) are necessary for the detailed analysis of plastic flow within the roll gap (Fig. 20.4).

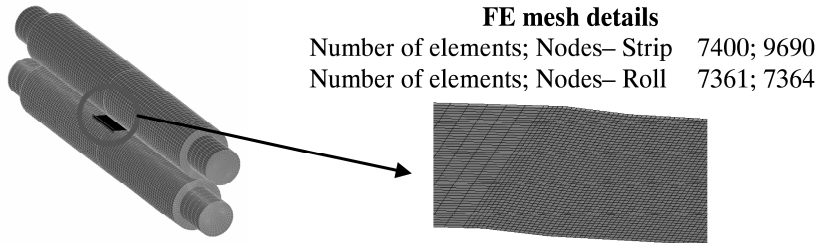

Fig. 20.4 FE mesh of the strip and work rolls for cold rolling simulations

To validate the simulation results obtained by the new modeling concept and to understand the underlying elastic-plastic strip material flow and elastic work roll deformation, cold rolling experiments were conducted on the rolling mill installed at IBF (Fig. 20.5 left). High-strength steel strips (ZStE340) with initial thicknesses of 1.67 mm were rolled to four different thickness reductions (Tab. 1).

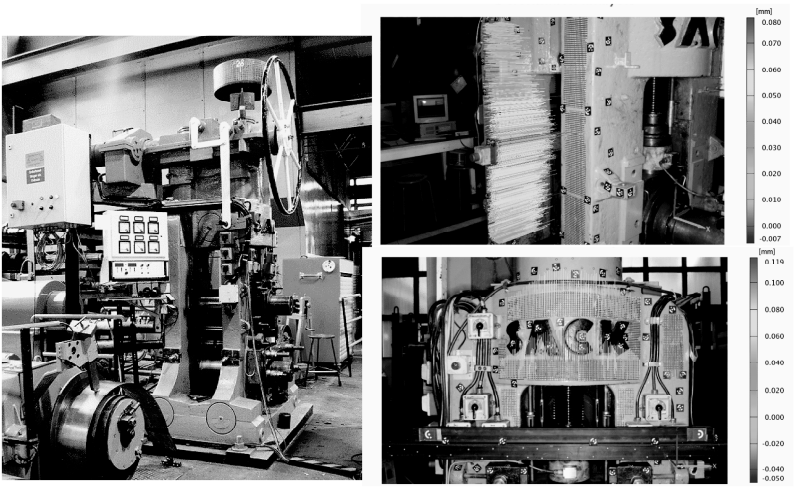

Fig. 20.5 Rolling mill installed at IBF (left), rolling mill deformation in rolling direction (top right) and in thickness direction (bottom right)

The rolling was conducted at a relatively low velocity 500 mm/s (conventional cold rolling velocity ranges 5 m/s up to 10 m/s) as the rolling mill limit is reached. For each case, the rolling force and the exit-strip thickness were measured. Furthermore, the elastic deformation of the whole mill was also measured using an optical measuring method TRITOP [38]. As shown in Figure 20.5, coded (fixed reference marks) and uncoded marks were placed on the rolling mill. At static loading conditions, free-form photographs were taken using a high resolution camera. With the help of the TRITOP software, the deformation of the uncoded marks was measured (see Fig. 20.5). As expected, the maximum deformation (0.12 mm) was observed in thickness direction whereas in the rolling direction the maximum deformation was observed as 0.08 mm.

20.3.1 Experimental and Simulation Results of Cold Rolling Process

The cold rolling process under consideration was simulated in 3D configuration using a non-linear implicit FE solver LARSTRAN/SHAPE. To obtain reliable steady state results, at least 150 mm strip length (~15 contact lengths) was simulated. As expected, the rolling force predicted using an elastic work rolls model is very close to the measurement (see Fig. 20.6). At the same time, the measured exit strip thickness also matches the simulated results very well. For the analysis of the strip thickness profile, the contact pressure distribution along the strip width was examined. It is clear from Figure 20.6 (bottom left) that the contact pressure distribution has a non-uniform profile in the elastic work roll model, which may lead to a non-uniform stress distribution within the roll gap. This directly influences the exit strip thickness. As shown in Figure 20.6 (bottom right), the equivalent plastic

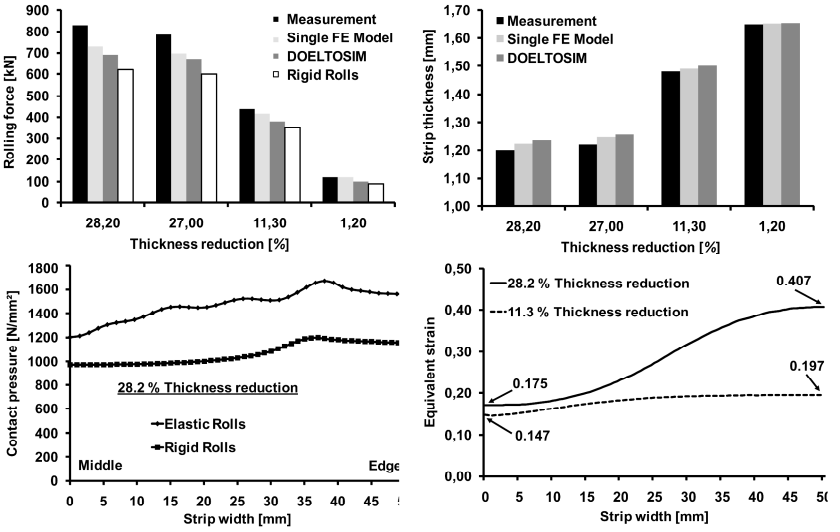

Fig. 20.6 Comparison of rolling force and exit strip thickness

strain along the strip width is not uniform (for high thickness reduction case), which confirms the non-uniform exit strip thickness for a 28.2 % thickness reduction case. Whereas for a low thickness reduction case, the plastic strain along the strip width is relatively uniform, this will lead to a uniform thickness reduction.

For the analysis of the plastic flow of the strip the comprehension of the shear stress distribution is very important. As shown in Figure 20.7 (left), there is a small "no-slip-zone" in the 28.2 % thickness reduction case. This means that there will be no significant thickness reduction in that region, whereas in a 14 % thickness reduction case (Fig. 20.7 - right) there is no such zone. From the Figures, it is clear that the plastic flow using the new modeling concept is identical to the single FE model. It can also be observed that the rolling force in the new model is smaller than in the single FE model, which may be due to a lower contact length in the new model. This directly depends on the frequency of the activation of the elastic roll model. This situation can be improved by increasing the activation of the tool simulation model, which may lead to a higher computation time. A compromise has to be found between these two phenomena to achieve reliable results. Detailed explanation regarding the frequency of the activation of tool simulation is given in [20].

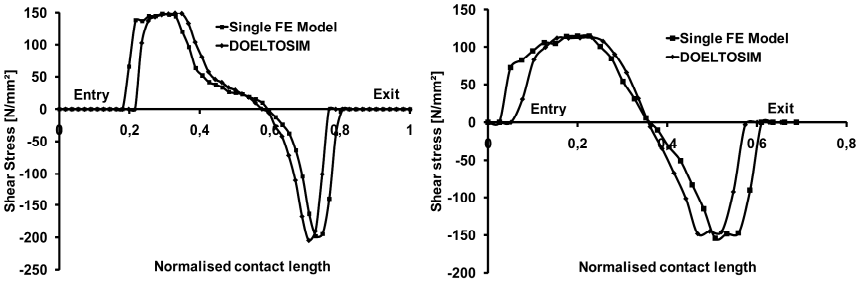

Fig. 20.7 Comparison of shear stress distribution (28.2 %, 11.3 %)

Any change in the work roll profile will directly affect the end strip quality. In order to control the required output strip specifications a careful analysis of the roll deformation is the key. Figure 20.8 shows the stress distribution in the strip thickness direction for a 23 % thickness reduction case predicted using LARSTRAN and ABAQUS [36].

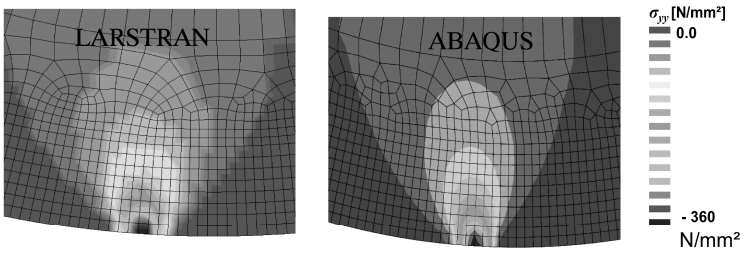

Fig. 20.8 Comparison of elastic stress distribution in work rolls

In both cases, the maximum compressive stress is about 360 N/mm², which is considerably lower than the yield stress of 860 MPa of the roll material. For the de-coupled simulation, a total of 200 coupled cycles were used and the computation time is up to 2 times faster than the single FE model. The computation time for the single FE model was about 614 minutes, whereas with the new concept (using DOELTOSIM module), it required only 316 minutes. From Figure 20.8 it is clear that the developed modeling concept is reliable and faster. Further details of the elastic roll influence on cold rolling process are explained in [19, 20].

20.4 Modeling and Analysis of Hot Rolling Process

In the hot rolling process, a large amount of heat energy is conducted into the work rolls during the contact with the hot strip. At the same time, the temperature distribution of the work rolls influences the forming characteristics of the strip. To analyze these interdependent phenomena, lab scale experiments and numerical simulations were conducted. Single-pass hot rolling experiments were conducted using 1.4301 stainless steel strips with an initial thickness of 1.9 mm and 150 mm width. The strip material flow curve was determined (using Eq. 20.10) for different strain rates and temperature up to strip inlet temperature, i. e >1,050°C. The strip material properties and rolling parameters are given in Table 2.

$$k_f = K.\dot{\varphi}^{(A+B.T)}.e^{C.T}.\varphi^{D}.e^{E.\varphi}$$
$$K = 7140.64 \text{ N/mm}^2,\ A = -0.26,\ B = 0.0004 \text{ 1/°C},\ C = -0.0033 \text{ 1/°C},\ D = 0.223,\ E = -0.62 \tag{20.10}$$

The strips were heated up to 1,050°C and rolled with a relatively low velocity of 200 mm/sec to two different thickness reductions (21 % and 26 %). To get a system level understanding, the rolling force was measured with high accuracy. To understand the heat transfer phenomenon the analysis of strip temperature distribution at the roll gap is an important aspect. It was not possible to measure the temperature distribution of the strip within the roll gap, it was, however, measured before and after the roll gap using pyrometers, as shown in the experimental setup (see Fig. 20.9).

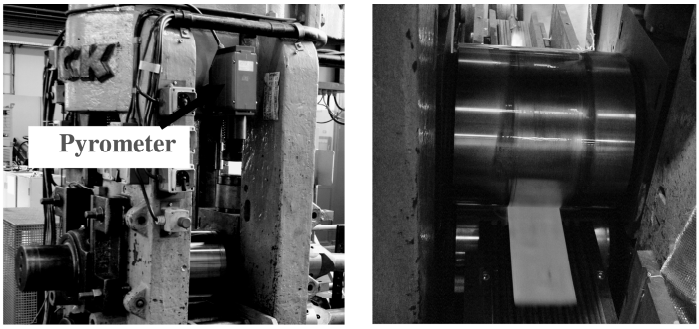

Fig. 20.9 Pyrometer setup for hot rolling experiments

The quality of the measured temperature using the pyrometer lies in the definition of the emission coefficient. The pyrometer was trained to obtain the precise coefficient using an additional experiment, where a specimen connected with a thermo-couple and the temperature was measured using both systems. Once both systems were measuring the identical temperature, the pyrometer was used in the real experiments. For the analysis of the strip temperature within the roll gap extensive numerical simulations were conducted.

In order to study the effects of the transient heat transfer phenomenon at the roll gap a good understanding of the process parameters is critical. For that purpose, numerical simulations were conducted using the newly-developed modeling concept. Within this concept, the process simulation was modeled using thermo-mechanical strip and the work rolls were modeled as rigid bodies. Although the roll was modeled as a rigid body the solver will consider the temperature distribution of the roll for solving the heat transfer at the roll gap. The work roll temperature will be updated using an external work roll model.

Table 20.2 Hot rolling process parameters and material properties

Roll geometric parameters		**Strip geometric parameters**	
Diameter	300 mm	Initial thickness	1.9 mm
Length	1,000 mm	Exit thickness	1.5,1.4 mm
Velocity	200,400,1000 mm/s	Width	150 mm
Roll material properties		**Strip material properties**	**Units**
Elastic	215E3 at 20 °C	198.340E3 at 20 °C	N/mm²
modulus	169E3 at 600 °C	117.000E3 at 1,000 °C	
Density	7.8E-9 at 20 °C	7.68E-9 at 500°C	Kg/mm³
	7.6E-9 at 600 °C	7.55E-9 at 1,000°C	
Conductivity	48.0 at 20 °C	14.85 at 20 °C	W/mm K
	44.3 at 600 °C	27.35 at 1,000 °C	
Specific heat	4.6E8 at 20 °C	4.55E8 at 20°C	J/Kg K
	5.9E8 at 600 °C	5.85E8 at 1,000 °C	

For the detailed analysis of the heat transfer phenomenon at the roll gap, the definition of gap conductance is most critical. Tseng [21, 22, 23] reviewed various analytical models for the definition of gap conductance and mentioned two sophisticated relations. The first is based on the analysis by Mikic [24] (Eq. 20.10), the second was semi-empirically derived by Yovanovich et. al. [25] (Eq. 20.11). In both Equations, k_h is the harmonic mean thermal conductivity in W/mm K, R_a is the combined arithmetic surface roughness in mm, P is the contact pressure and M is the hardness of the softer material. For hot rolling, the analysis of thermal contact conductance of the interface should include the conductance of oxide scale. To serially link the oxide layer with interface contact conductance, the conductance in Equations 20.11 and 20.12 can be modified as shown in Equation 20.13, where the underline signifies the contact conductance including the oxide scale conductance, which equals k_0/δ_0. Here, k_0 and δ_0 are the thermal conductivity and

thickness of oxide scale respectively. The properties of the oxide layer during the hot rolling of various grades of steels were studied in detail by the large number of researchers [26, 27, 28]. Conventionally, high pressure jets are used to desiccate between the stands so that the scale layer is kept relatively thin. A 10 µm oxide layer is consistent with most measurements [27, 28]; and the hardness of the oxide layer was observed as 980 MPa (HV100). A user sub-routine was developed (and implemented in a model program for PEP) to define the gap conductivity according to Equation 20.13, where the local contact pressure is extracted from the process simulation. With this, a detailed analysis of heat transfer between work roll and strip was conducted.

$$h_c = 3800 k_h R_a^{-0.257} \left[P/(M+P)\right]^{0.95} + \left(k_m/\delta_m\right) r_{unc} \tag{20.11}$$

$$h_c = 4200 k_h R_a^{-0.257} \left[P/M\right]^{0.95} + \left(k_m/\delta_m\right) r_{unc} \tag{20.12}$$

$$\underline{h}_c = h_c \left(k_o/\delta_o\right) / \left[h_c + \left(k_o/\delta_o\right)\right] \tag{20.13}$$

Furthermore, it is important to analyze the thermo-mechanical behavior of the work rolls during the hot rolling process. The work rolls are heated during the contact with the strip by conduction, which is predominant in the hot rolling process [29]. The heating of the rolls is countered by the proper cooling system, which is normally provided by water sprinklers located at the entry and exit side of the stand (Fig. 20.10). The rolling velocity and the angle the cooling (on both sides) is provided at determine the temperature distribution and also the surface stresses of the work rolls. To analyze these aspects a rotating boundary concept was introduced. To determine steady state temperature distribution within the work rolls various parameter variations were tested and qualitative results will be presented in the next section.

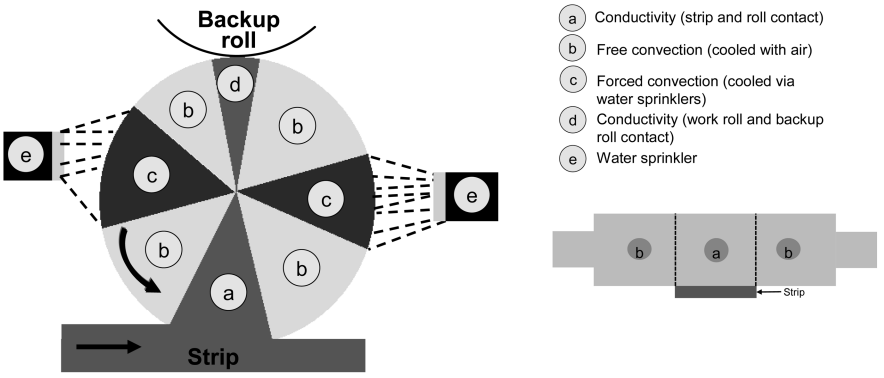

Fig. 20.10 Boundary conditions for work rolls during hot rolling process

20.4.1 Experimental and Simulation Results of Hot Rolling Process

Various hot rolling experiments and simulations were conducted to analyze the heat transfer phenomenon between the hot strip and the work roll. Coupled thermo-mechanical simulations were conducted using the non-linear implicit solver LARSTRAN/SHAPE [37]. The computation of roll thermal effects is conducted in a separate simulation model and coupled with the process simulation using the newly-developed module DOHOTSIM. Transient 3D thermo-mechanical simulations were conducted with the rolling process data given in Table 2. The rolling force measured was about 750 kN and 850 kN for 21 % and 26 % thickness reductions respectively. Since the strip surface roughness was high, using a high-friction coefficient (μ=0.6) and with the pressure-dependent gap conductance, the predicted rolling force was about 735 kN and 837 kN for 21 % and 26 % thickness reduction cases respectively. For the analysis of plastic flow in the roll gap, the shear stress was analyzed under two different aspects.

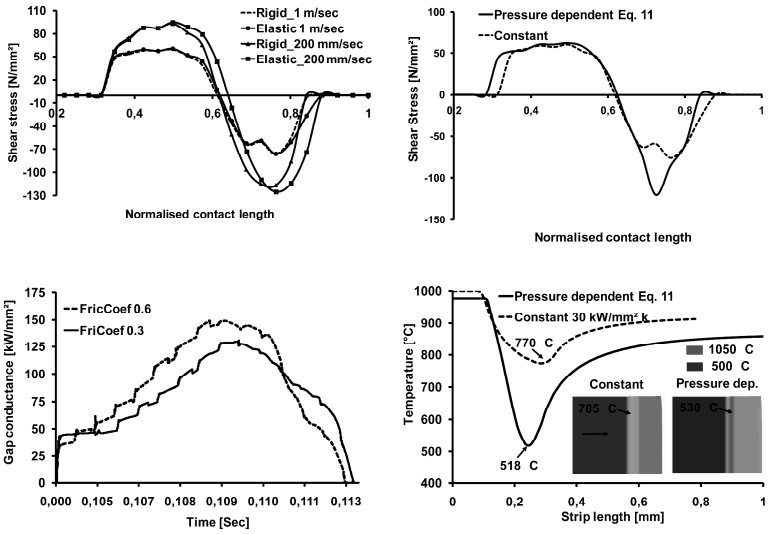

Fig. 20.11 Strip shear stress and temperature distribution in hot rolling

The first one is the influence of elastic tool effects and the second the definition of gap conductance. The shear stress as shown in Figure 20.11 (top left) is predicted for two different rolling velocities, both using rigid and elastic rolls for 21 % thickness reduction case. For a high velocity, low shear stress is predicted and vice versa. This may directly depend on the strip temperature distribution. At the same time, the influence of the elastic work roll on the plastic deformation of the strip is considerably low. However, the influence of the definition of gap

conductance on the plastic deformation has a considerable effect (Fig. 20.11, top right). On the entry side, the shear stress distribution has identical behavior in both models whereas on the exit side, the pressure-dependent model predicts high shear stresses. This may be due to the tendency in the strip temperature in both models.

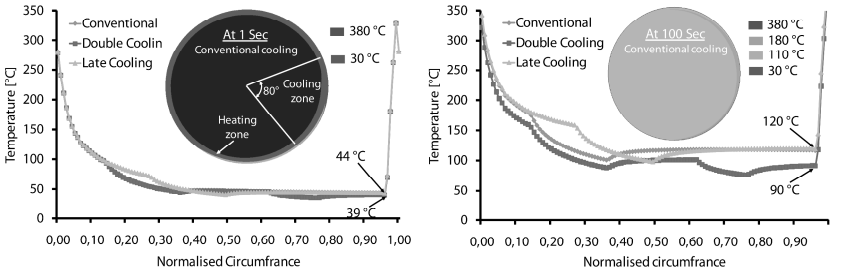

Fig. 20.12 Surface temperature distribution of the work roll for first rotation (left) and after 100 sec (right)

For the clear understanding of the heat transfer between strip and work roll, a pressure-dependent gap conductance was defined according to Equation 10. Figure 20.11 (bottom left) shows the predicted gap conductance (for two different friction coefficients) for a node as it passes through the roll gap. From the Figure, it is clear that the gap conductance has a profile identical to the contact pressure distribution and reaches its maximum at the exit side of the roll gap, where the normal compressive contact pressure has its maxima. Figure 20.11 (bottom right) makes it clear that the strip temperature predicted using both models before and after the roll gap matches well with the measured temperature (755 °C). An important phenomenon can be observed here: the strip temperature along the roll gap has a large deviation (pressure-dependent model predicts up to 230 °C lower than the constant gap conductance model- see Fig. 20.11) in both models. Neglecting this phenomenon during the modeling of a hot rolling process may lead to serious problems since the metallurgical changes directly depend on the forming temperature and others [30, 31].

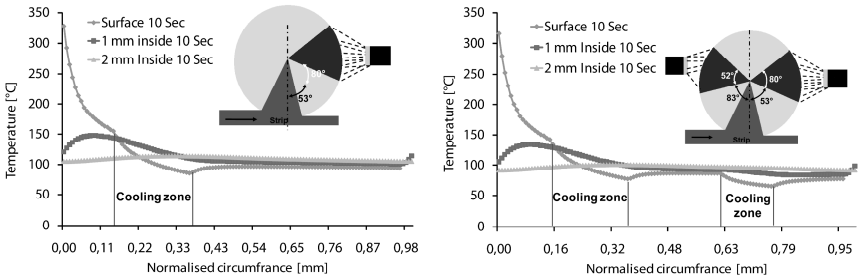

Fig. 20.13 Temperature distribution at surface and inside the roll (left - conventional cooling, right - double cooling)

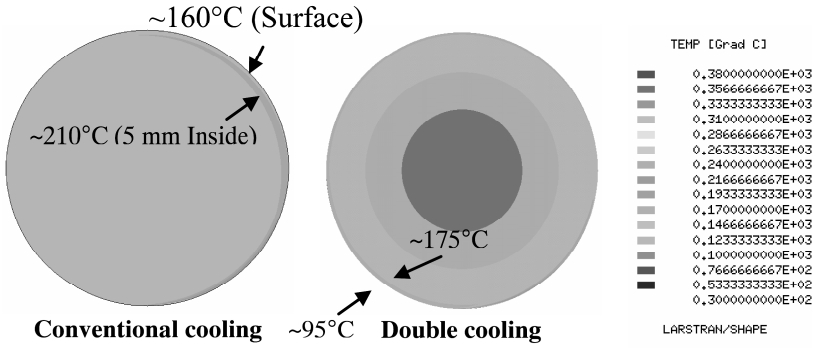

Fig. 20.14 Temperature distribution at the surface and inside the roll

A detailed analysis of the thermal evolution of the work rolls is very important since the life and the wear of the work rolls can be controlled by improving the cooling system [32, 33]. The proper cooling may reduce the induced thermal stresses and, from that, the abatement of the thermal fatigue may be achieved. To understand this phenomenon, a new rotating boundary model was developed and implemented within the FE program PEP [39] and LARSTRAN. For the qualitative numerical analysis, the hot rolling lab experiments were modeled assuming different cooling strategies. Figure 20.12 shows the temperature evolution at the surface of the roll for the first rotation (left) and after 10 seconds of rolling (rolling velocity 1 m/sec) for three different cooling strategies (conventional, double cooling and late cooling [33, 34]). The schematic diagram of the first two strategies is shown in Fig. 20.13 and the late cooling means that the cooling starts at 130°). From the first rotation curves for all cooling methods it can be observed that due to insufficient cooling a small amount of heat (about 15°C) is retained in the work rolls. After 100 seconds of rolling, the temperature distribution has a clear difference (up to 30 °C) between double and conventional cooling methods. The steady state thermal evolution (Fig. 20.13) confirms that the thermal gradient produced during one cycle is restricted to the surface of the roll. One more important phenomenon can be observed in these figures, i. e. the temperature on the surface at some angular positions is cooler than the core and in other locations hotter than the core. This leads to tensile stresses at cooler locations and compressive stresses at the hotter locations, which may cause the fire-cracks on the surface of the rolls.

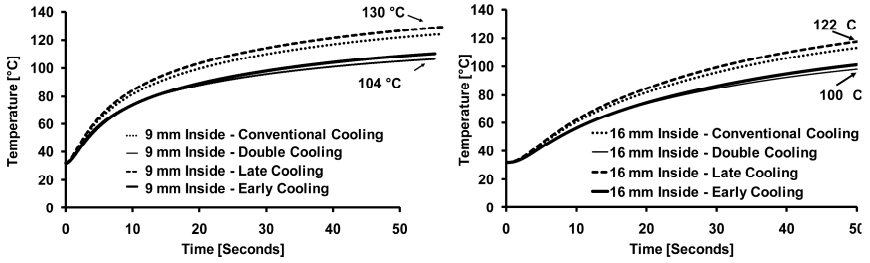

Fig. 20.15 Penetration of temperature for different cooling methods

To understand the cooling efficiency and the resulting thermal effects the history of the temperature penetration for various cooling strategies has to be examined. Figure 20.14 and 20.15 show the thermal evolution of the work rolls for four different cooling methods at two different locations (9 and 16 mm inside). From the Figures it is clear that the double cooling phenomenon slows down the penetration of the thermal gradient and less heat is retained in the rolls after each rotation.

20.5 Work Roll Wear Modeling and Simulation Results

The most important tribological effect, which influences the exit strip thickness profile is work roll wear. During a cold rolling process, due to very high quality tolerances, macroscopic wear of the work rolls may not be observed since the rolls are changed frequently after a defined roll surface roughness. During hot rolling process (particularly the continuous strip casting mill), however, the work roll wear is more significant and mostly not uniform along the strip width [12,13]. Figure 20.16 shows a typical wear profile of a work roll [35], where the wear at the edges of the strip is considerably higher than the middle. This might be because of the non-uniform temperature (particularly cooled edges) of the incoming strip [34], which results in high contact pressure at the edges. The middle wear, however, is relatively homogeneous. For the analysis of the wear profile, various analytical wear models have been developed and are also being used for on-line observations [11, 12, 13]. The major drawback of most of the models is that they are not suitable for the prediction of local effects but useful to get the average value (along the strip width direction) of the wear [13, 14]. It is also necessary to understand the phenomenon of local wear for the better planning of the scheduling and roll change.

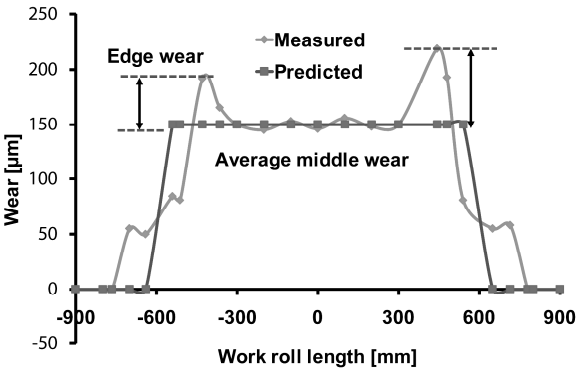

Fig. 20.16 Typical work roll wear profile during hot rolling process (Stand 5)

Within this work, a decoupled modeling concept was introduced for the prediction of local work roll wear during cold and hot rolling process. As described in the concept and implementation section, three different wear models were implemented to analyze the work roll wear effects on the rolling process. The models were validated by the published data [13, 18]. In particular, Sikdar [18] published hot rolling process information and the measured work roll wear for the finishing stands. Within their work, the roll surface profile was measured before and after a rolling schedule using a contact type profile gauge with a measuring accuracy of ± 1 μm. After rolling a selected number of strips (for the published case, 56 strips), the worn work rolls were removed from the finishing mill and subjected to 2h of water cooling followed by 3h of air cooling. This cooling schedule eliminated any effects of thermal expansion on the work rolls. The other source used for the validation was published by Mohammed Tahir [13], where the wear of the work rolls was evaluated for different roll materials for hot rolling finishing mills. According to this input, various simulations were conducted to understand the work roll wear using three different wear models and compared with the published data. The work roll wear of the finishing stand (stand 4, top roll) of a tandem rolling mill was further analyzed. The process conditions at this stand are provided in [18]. Three different strip widths (900, 700 and 500 mm) were simulated for the strip length of 100 km each. The average simulated rolling force (for three strips) was about 13.5 MN whereas the measured force ranges at about 12.5 MN [18].

For the analysis of wear using the empirical model (Eq. 6), the coefficients α, β and γ were 1.0E-10, 0.188 and 0.11 respectively. To predict wear the normal pressure is obtained from the process simulation and Equation 6 solved for each surface element. As shown in Figure 20.17, for the work roll wear profile at the centre, i. e. up to 500 mm, the wear is higher and uniform. The reason is that, for all strip widths, the work roll is loaded at the centre. When using an empirical wear model, the wear along the strip width is uniform; the reason for this could be that the model considers only the normal contact pressure. Another cause may be the inlet strip temperature, which is assumed to be uniform over the width, and there is no considerable elastic deformation of the work rolls, which influence the contact pressure profile. Figure 20.17 (right) shows the contact pressure distribution (for 700 mm strip width) before and after updating the worn roll profile within the process simulation.

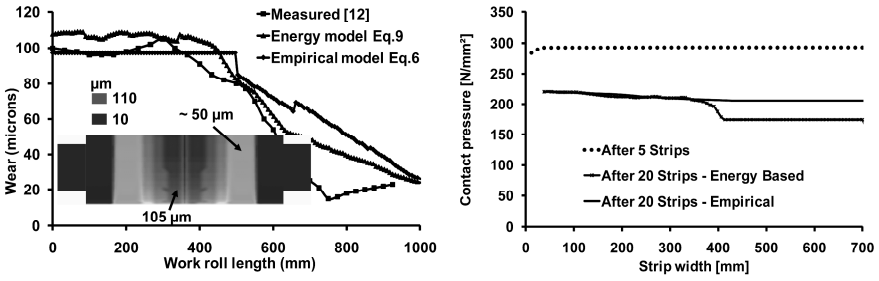

Fig. 20.17 Comparison of work roll wear for roll stand 4

Since the stresses due to friction are relatively high during the rolling process any prediction neglecting these may lead to undesired results [17]. For that, an energy-based wear model was implemented, which considers the frictional dissipation rate. For each element, the accumulated wear work is estimated. The required shear stress and the normal stresses are extracted from the process simulation. The relative velocity in rolling direction is the difference of the roll velocity and the strip velocity within the roll gap. Using this information, wear Equation 10 is solved for each surface element. As shown in Figure 20.17, the wear predicted by the energy model is relatively local and higher than empirically estimated at the middle, where high shear stresses may occur. The order of magnitude from both models is very close to the measured wear profile. Further analysis and the validation of these models have to be conducted with real experimental data.

20.6 Conclusion and Outlook

A new FE modeling concept was developed for the analysis of interaction effects during the flat rolling process. Within this concept, the tool simulation is separated from the process simulation and, using an automatic coupling module, the communication between these two models was realized. The advantages of this modeling concept includes a short computation time (up to 2 times faster than a single FE model in the case of an elastic tool model) compared to the single FE model, suitable for the analysis of flatness problems (modeling of 3D), easy to handle thermo-mechanical effects during the modeling of a hot rolling process and the influence of tribological effects (particularly abrasive wear of the work rolls) on the strip quality can be analyzed. The simulation results of the cold rolling process (with the careful selection of frequency of activation of the tool computation) show good agreement with the single FE model and also the experiments. At the same time, the modeling of the hot rolling process was also validated with the help of lab experiments. The rolling force was clearly underestimated using a constant gap conductance model, even with a high friction coefficient. When using the pressure-dependent model, however, the predicted rolling force is very close to the measured value. At the same time, the exit strip temperature and strip exit thickness also matches well with the measurements. For the analysis of roll thermal events for different cooling strategies, extensive numerical analysis was conducted using the rotating boundary model. It was shown that the model is suitable and easy to handle for the prediction of steady state thermal gradients within the work rolls.

At the end, wear models were validated using published data. Since the history of the rolled strip width is not mentioned within the publication, further analysis and validation of the simulated results are necessary. Future work will consider obtaining precise wear data from the industry to validate the developed models.

References

[1] Kainz, A., Krimplelstätter, K., Zemen, K.: FE Simulation of thin strip and temper rolling processes. In: ABAQUS Austria User Conference (2003)
[2] Kim, T.H., Lee, W.H.: An integrated FE process model for the prediction of strip profile in flat rolling. ISIJ 43, 1947–1956 (2003)
[3] Ohe, K., Kajiura, S., Simada, S., Mizuta, A., Morimoto, Y., Fujino, T., Anraku, K.: Development of shape control in plate rolling. In: METEC Conference proceedings, vol. 2, pp. 78–85 (1994)
[4] Buessler, P., Montmitonnent, P.: A review on theoretical analysis of rolling in Europe. ISIJ 31, 525–538 (1991)
[5] Guo, R.-M.: Development, verification and application of an optimal crown shape control model for rolling mills with multiple control devices. In: AISE Conference (1995)
[6] Tseng, A.A.: A numerical heat transfer analysis of strip rolling. ASME 106, 512–517 (1984)
[7] Hsu, C.T., Evans, R.W.: Finite element analysis on the hot rolling of steel. Adv. Tech. Plasticity 2, 587–593 (1990)
[8] Sun, C.G., Hwang, S.M.: Prediction of roll thermal profile in hot strip rolling by the Finite element method. ISIJ 40, 794–801 (2000)
[9] Sun, C.G., Hwang, S.M., Ryoo, S.R., Kwak, W.J.: An integrated FE process model for precision analysis of thermo-mechanical behaviour of the rolls and strip in hot strip rolling. Comp. Methods. Appl. Mech. Engg. 191, 4015–4033 (2002)
[10] Lee, J.H., Hwang, S.M., Park, H.D.: FE-based on-line model for the prediction of roll force and roll power in hot strip rolling. ISIJ 40, 1013–1018 (2000)
[11] Jiang, Z.Y., Tieu, A.K.: Contact mechanics and work roll wear in cold rolling of thin strip. Wear Journal 263, 1447–1453 (2007)
[12] Magne, A., Gaspard, C., Gabriel, M.: Wear behaviour of steels for hot working rolling-mill rolls. CRM 57, 25–39 (1980)
[13] Mohammed, T., Widell, B.: Roll wear evaluation of HSS, HiCr and IC work rolls in hot strip mill. Steel Research 74, 624–630 (2003)
[14] Kivilcim, E.N., Nürnberg, G., Golle, M., Hoffmann, H.: Simulation of wear on sheet metal forming tools—An energy approach. Journal of Wear, 357–363 (2008)
[15] Archard, J.F., Hirst, W.: Wear of metals under un-lubricated conditions. Proceedings of the Royal Society of London 236, 397–410 (1956)
[16] Byon, S.M., Kim, S.I., Lee, Y.: A semi-analytical model for predicting the wear contour in rod rolling process. Journal of Materials Processing Technology 191, 306–309 (2007)
[17] Bowden, F.P., Tabor, D.: Friction, lubrication and wear: a survey of work during the last decade. British Journal of App. Physics 17, 1521–1544 (1966)
[18] John, S., Sikdar, S., Mukhopadhyay, A.: Roll wear prediction model for finishing stands of hot strip mill. Iron and Steel Making 33, 169–175 (2006)
[19] Franzke, M., Puchhala, S., Dackweiler, H.: Modeling of interaction effects between strip and roll during flat rolling process. In: NUMIFORM Conference Proceedings, vol. 908, pp. 1489–1494 (2007)
[20] Franzke, M., Puchhala, S., Dackweiler, H.: Modeling of interaction effects between process and machine during flat rolling process. In: PMI Conference Proceedings (2008)

[21] Tseng, A.A., Huang, C.H.: The estimation of surface thermal behavior of the working roll in hot rolling process. Heat and Mass Transfer 18, 1019–1031 (1995)
[22] Tseng, A.: Thermal modeling of roll and strip interface in rolling process: part 1 – review. Numerical Heat Transfer 35, 115–135 (1999)
[23] Tseng, A.: Thermal modeling of roll and strip interface in rolling process: part 2 – review. Numerical Heat Transfer 35, 135–154 (1999)
[24] Mikic, B.B.: Thermal contact conductance: Theoretical considerations. International Heat Transfer 17, 205–214 (1974)
[25] Yovanovich, M.M., De Vaal, J., Hegazy, A.: A statistical model to predict thermal gap conductance between conforming rough surfaces. AIAA Paper No: 82-0888 (1998)
[26] Colas, R., Torres, M.: Modeling heat conduction through an oxide layer during hot rolling of steel. ASME Manufacturing Science Engineering 68(2), 577–582 (1994)
[27] Browne, K.M., Dryden, J., Assefpour, M.: Modeling scaling and de-scaling in hot strip mills. Recent Advances in Heat Transfer and Micro Structure Modeling for Metal Processing 67, 187–201 (1995)
[28] Ranta, H., Larkoila, J., Korhonen, A.S.: A study of scale effects during accelerated cooling. In: Modeling of Metal Rolling Process Conference Proceedings, pp. 638–647 (1993)
[29] Tseng, A.A.: A numerical heat transfer analysis of strip rolling. ASME Journal of Heat Transfer 106, 512–517 (1984)
[30] Sellars, C.M., McLaern, A.J.: Modeling distribution of microstructure during hot rolling of stainless steel. Materials Science and Technology 8, 1090–1095 (1975)
[31] Militzer, M., Nakata, N.: Modeling of microstructure evolution during hot rolling of a 780 MPa high strength steel. ISIJ 45, 82–90 (2005)
[32] Tseng, A.A., Lin, F.H., Gunderia, A.S., Ni, D.S.: Roll cooling and its relationship to roll life. Metallurgical Transactions 20A, 2305–2320 (1988)
[33] Sun, C.G., Hwang, S.M.: Prediction of roll thermal profile in hot strip rolling by the FE Method. ISIJ 40, 794–801 (2000)
[34] Azene, Y.T., Roy, R., Farrugia, D., Onisa, C., Trumann, M.H.: Work roll cooling system design optimization in presence of uncertainty. In: CIRP Design Conference Proceedings, pp. 57–65 (2009)
[35] Partender, E., Mitter, S.: Ein Modell zur Prognose des Arbeitswalzenverschleiß der Breibandstraße in Linz. In: XXII Verformungskundlisches Kolloquium (2003)
[36] Simulia, http://www.simulia.com/products/abaqus_fea.html
[37] Lasso GmBh, http://www.lasso.de/index.php?id=28
[38] GOM, Optische 3D-Koordinatenmessmaschine http://www.gom.com/de/messsysteme/systemuebersicht/tritop.html
[39] Franzke, M.: Zielgrößenadaptierte Netzdiagnose und -generierung zur Anwendung der Finite Elemente Methode in der Umformtechnik. Dissertation, RWTH Aachen University (1999)